Biophysical Chemistry 156 (2011) 128–139

Contents lists available at ScienceDirect

Biophysical Chemistry

journal homepage: http://www.elsevier.com/locate/biophyschem

Spectroscopic probe analysis for exploring probe–protein interaction: A mapping of native, unfolding and refolding of protein bovine serum albumin by extrinsic fluorescence probe

Anuva Samanta, Bijan Kumar Paul, Nikhil Guchhait *

Department of Chemistry, University of Calcutta, 92 A.P.C. Road, Kolkata 700009, India

ARTICLE INFO

Article history:
Received 28 January 2011
Received in revised form 7 March 2011
Accepted 24 March 2011
Available online 5 April 2011

Keywords:
Bovine serum albumin
para-N,N-dimethylamino orthohydroxy benzaldehyde
Fluorescence spectroscopy
Circular dichroism
Energy transfer
Denaturant

ABSTRACT

Steady state and dynamic fluorescence measurements have been used to investigate interaction between Bovine Serum Albumin (BSA) and fluorescence probe para-N,N-dimethylamino orthohydroxy benzaldehyde (PDOHBA), a structurally important molecule exhibiting excited state coupled proton transfer (PT) and charge transfer (CT) reaction. Fluorescence anisotropy, acrylamide quenching, and time resolved fluorescence measurements corroborate the binding nature of the probe with protein. The binding constant between BSA and PDOHBA has been determined by using Benesi–Hildebrand and Stern–Volmer equations. The negative value of ΔG indicates the spontaneity of this probe–protein complexation process. Observations from synchronous, three dimensional fluorescence spectra and circular dichroism spectra point toward the fact that the hydrophobicity as well as α-helix content of BSA are altered in presence of probe PDOHBA. The PT band of PDOHBA is found to be an excellent reporter for the mapping of destructive and protective behavior of SDS with variation of chaotrope concentration.

1. Introduction

Serum albumins are the most abundant proteins in the circulatory system of different organisms, being the major macromolecule contributing to the osmotic blood pressure [1,2]. The most vital property of this group of proteins is that they serve as depot protein and transport protein for a variety of compounds like fatty acids, amino acids, bile salts, metals, hormones, drugs and pharmaceuticals [1,3–8]. The nature of binding between small molecular probes and albumins is an interesting research field in chemistry, life sciences and clinical medicine for many years [9–11]. Bovine serum albumin (BSA) is a model protein with stability, water solubility and unusual binding capacity [12] and has structural homology with human serum albumin (HSA). The protein BSA, with a molecular mass of 66,200 Da, having 583 amino acids in a single polypeptide chain [13], is made up of three homologous domains (I, II, and III) divided into nine loops (L1–L9) by 17 disulphide bridges. Each domain in turn is the product of two sub-domains [14]. BSA has two tryptophan residues that possess intrinsic fluorescence. Trp-212 locates within a hydrophobic binding pocket in the subdomain IIA, and Trp-134, locates on the surface of the albumin molecule in domain I [2].

One of the major endeavors in molecular biology is to study the mechanism behind surfactant induced protein folding/unfolding/refolding process [15]. Small changes in the local environment of a protein may cause structural changes, thereby affecting the original function of the protein. Rare neurodegenerative illnesses like Alzeimer's, Parkinsons etc. are the effect of unusual folding behavior of protein [16,17]. So considerable attention has been devoted on the interaction between ionic surfactants and globular proteins as binding of ionic surfactant molecules to proteins disrupts the native structure of most globular proteins [18,19]. The interaction between sodium dodecyl sulfate (SDS) and BSA is often used as an archetype system [18–23] as SDS binds very strongly to BSA and serves as an effective stabilizing and destabilizing agent.

Traditional ways such as Bradford method, Lowry method and Biuret method are used for the study of proteins and these methods are generally based on absorption spectroscopy [24–26]. Fluorescence spectroscopy serves as a feasible and powerful sensing tool for the investigation of local environment of the fluorophore yielding structural and dynamical information concerning the fluorophore environment [27–29]. Extrinsic fluorescence probe such as excited state charge, proton and electron transfer molecules can be used successfully for studying conformational changes of protein structure with variation of its solvent characteristics [30–35]. The molecule para-N,N-dimethylamino orthohydroxy benzaldehyde (PDOHBA) is one of the interesting organic molecule studied by our group which exhibits excited state coupled intramolecular charge transfer (CT) and

* Corresponding author. Tel.: +91 33 2350 8386; fax: +91 33 2351 9755.
E-mail address: nguchhait@yahoo.com (N. Guchhait).

0301-4622/$ – see front matter © 2011 Elsevier B.V. All rights reserved.
doi:10.1016/j.bpc.2011.03.008

proton transfer (PT) reaction [36]. Interestingly, in water, PDOHBA shows only large Stokes shifted PT emission band, but not the CT band. In the present work, we have explored the influence of hydrogen bonding on proton transfer emission band of PDOHBA to monitor the conformational changes of protein in absence and presence of surfactant and chaotropes. The quenching of the intrinsic tryptophanyl fluorescence of BSA has also been used as a tool to study the interaction of PDOHBA with this transport protein to characterize any conformational change of protein. Meanwhile, several measurements including fluorescence quenching, synchronous and three dimensional fluorescence spectra, and CD measurements are employed to achieve the binding constants, thermodynamic parameters and the structural changes of BSA.

2. Materials and methods

2.1. Reagents

The molecule PDOHBA (Scheme 1) was synthesized using simple literature procedure and has been described in our previous publication [36]. BSA, SDS and urea were purchased from SRL, India. Tris–HCl buffer (0.01 M, pH = 7.0) was prepared from Tris–HCl buffer purchased from SRL, India. Triple distilled water was used for the preparation of buffer solution. Acrylamide was used as received from SRL, India.

2.2. Fluorescence and UV–Vis absorption

The room temperature absorption and fluorescence spectra were recorded using Hitachi UV–Vis U-3501 spectrophotometer and PerkinElmer LS-55 fluorimeter, respectively. The width of excitation and emission slit was set to 5.0 nm in each case. For the fluorescence quenching phenomenon, the fluorescence spectra were measured (λ_{ex} = 295 nm) at three different temperatures (303 K, 308 K, and 313 K). Synchronous fluorescence spectra were recorded with $\Delta\lambda$ value between excitation and emission wavelength stabilized at 15 nm and 60 nm, respectively. The three dimensional fluorescence spectra were performed maintaining the following conditions: the emission wavelength was recorded between 200 and 500 nm. The initial excitation wavelength was set to 200 nm with increment of 5 nm and 30 scan. Steady state fluorescence anisotropy was measured using the same fluorimeter. The steady state fluorescence anisotropy, r, is defined by

$$r = \frac{(I_{VV} - G.I_{VH})}{I_{VV} + 2G.I_{VH}}. \quad (1)$$

Here, I_{VV} and I_{VH} are the emission intensities obtained with the excitation polarizer oriented vertically and emission polarizer oriented vertically and horizontally, respectively. The G factor is the ratio of sensitivities of detection systems for vertically and horizontally polarized light $G = I_{HV}/I_{HH}$.

The fluorescence quantum yields were estimated from the corrected fluorescence spectra using quinine sulfate in 0.1 M H_2SO_4 (Φ_F = 0.577 at 293 K) as secondary standard [37].

2.3. Fluorescence lifetime measurements

All the fluorescence decays were obtained with a Time Correlated Single Photon Counting (TCSPC) set up employing a nanosecond diode laser (IBH, nanoLED-07) operating at λ_{ex} = 340 nm as the light source and TBX-04 as the detector [38]. Instrument response function is 45 ps. The fluorescence decay was collected with an emission polarizer kept at the magic angle (~54.7°). The decays were analyzed using Data Station v-2.5 decay analysis software. The fluorescence decay curves were analyzed by tri-exponential fitting program of IBH in order to obtain best residuals and acceptable χ^2 values. Intensity decay curves were obtained as a sum of exponential terms

$$F(t) = \sum_i a_i \, exp\left(\frac{-t}{\tau_i}\right) \quad (2)$$

where F(t) is the fluorescence intensity at time t, and a_i the pre-exponential factor representing the fractional contribution to the time resolved decay of the ith component with a lifetime τ_i. Average lifetimes ($\langle\tau_{avg}\rangle$) of fluorescence were calculated from the decay times and pre-exponential factors using the following equation:

$$\langle\tau_{avg}\rangle = \sum_i a_i\tau_i \quad (3)$$

2.4. CD measurements

The alterations in the secondary and tertiary structure of the protein in the presence of the probe were studied by monitoring Circular Dichroism (CD) on Jasco Corporation, J-815 CD spectrophotometer using a rectangular quartz cuvette of path length 1.0 mm at 1 nm data pitch intervals. All CD spectra were taken in a wavelength range 200–350 nm. The spectrophotometer was sufficiently purged with 99.9% nitrogen before starting the instrument. The spectra were collected at a scan speed of 100 nm/min and a response time of 1 s. Each spectrum was baseline corrected and the final plot was taken as an average of three accumulated plots.

3. Results and discussion

3.1. Absorption and fluorescence spectra of PDOHBA

Before going to the study of interaction between fluorescence probe PDOHBA and protein BSA, it is worth to discuss briefly the spectral properties of probe molecule [36]. The targeted fluorescent molecule PDOHBA has donor–acceptor charge transfer site resemble to 4-dimethylaminobenzaldehyde (DMABA) molecule and proton transfer site resemble to ortho-hydroxybenzaldehyde (OHBA). From our previous publication [36] it is clear that the molecule shows a strong absorption peak at ~332 nm in nonpolar solvents which shifts to ~348 nm in water. The strong π–π* transition of PDOHBA correlates well with the absorption peaks of two subunits as DMABA shows π–π* transition at ~337 nm and the intramolecular hydrogen bonded closed form of OHBA shows peak at ~350 nm [39,40]. PDOHBA exhibits a large Stokes shifted fluorescence band at ~513 nm in nonpolar solvents as well as polar solvents [36]. It is to note that DMABA is nonfluorescent in nonpolar solvents [39]. A detailed spectral analysis indicate that the molecule PDOHBA shows only excited state intramolecular proton transfer (ESIPT) reaction in nonpolar solvents at ~513 nm and coupled

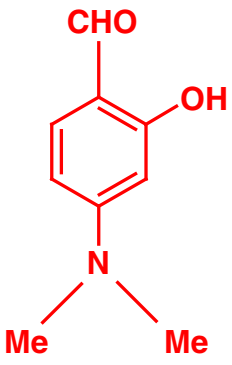

Scheme 1. Molecular structure of PDOHBA.

proton and charge transfer reaction in polar solvents (except water) at ~513 nm and ~550 nm respectively. In water, the molecule DMABA does not display charge transfer emission due to decrease of energy gap between the ICT state and the Franck–Condon state resulting in a rapid nonradiative decay of ICT state to the low lying triplet states [41]. The large Stokes shifted emission band at ~518 nm in water has been assigned to proton transfer emission from PDOHBA.

3.2. Binding study of PDOHBA with BSA

As shown in Fig. 1, the changes in the absorption and emission spectra of PDOHBA on addition of BSA reveal the interaction between two partners. It is clear from Fig. 1(a) that gradual addition of BSA to a solution of PDOHBA in aqueous buffer results in gradual shift of the absorption maxima to the red from ~348 nm in Tris buffer to ~353 nm in 40 μM BSA concentration. On the contrary, the position of the emission maxima show hypsochromic shift from ~515 nm (in buffer) to ~460 nm (40 μM BSA) with manifold enhancement of emission intensity by addition of BSA (Figs. 1(b) and 2(a)). This observation reflects that the microenvironment around the fluorophore in protein solution is quite different from that in pure aqueous phase. Usually such type of blue shift of the emission maxima of the PT band of PDOHBA indicates that the probe molecule is encapsulated inside the hydrophobic cavity of the protein. It is already mentioned in the previous publication [36] that the fluorescence quantum yield of PDOHBA in highly polar solvents like water is low compared to that in somewhat less polar medium. Hence, the increase in intensity and fluorescence quantum yield value (Table 1) on addition of protein

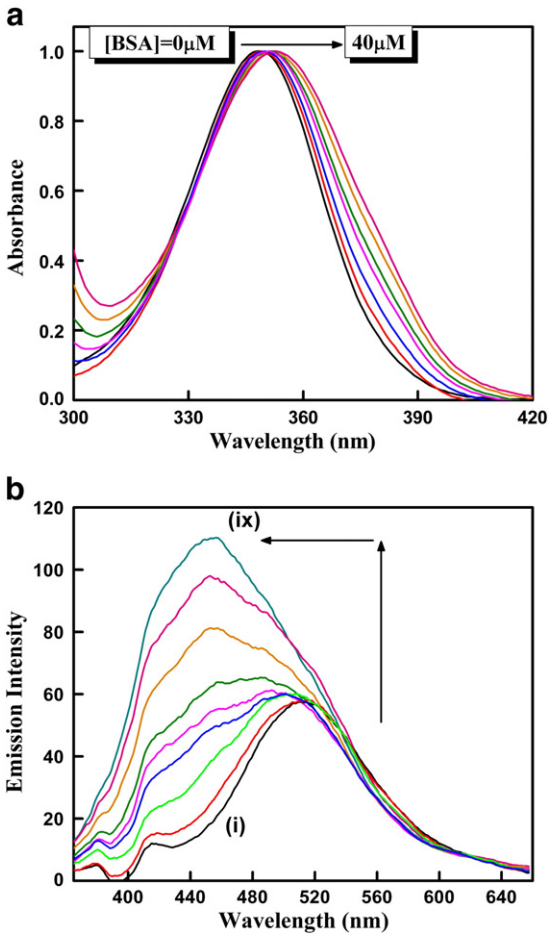

Fig. 1. Effect of increasing concentration of BSA on the (a) absorption ([BSA] = 0, 3, 7, 13, 20, 30 and 40 μM) and (b) fluorescence emission spectra (λ_{ex} = 350 nm) of PDOHBA ([PDOHBA] = 6 μM, [BSA] = 0, 3, 7, 13, 16, 20, 27, 30 and 40 μM).

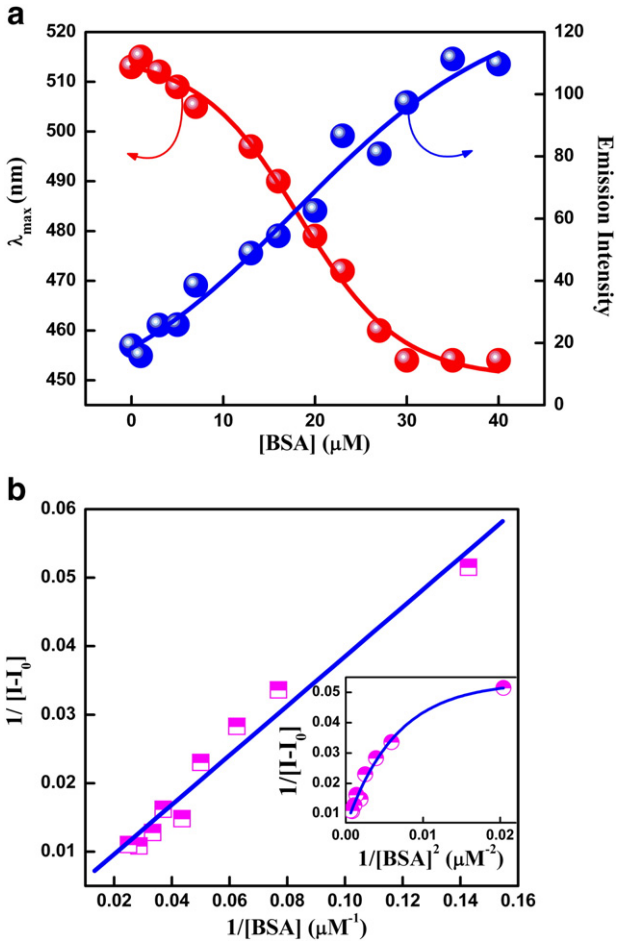

Fig. 2. (a) Plot of the emission intensity and emission maxima (λ_{max}) of PDOHBA with increasing concentration of BSA. (b) Benesi–Hildebrand plot of $1/(I-I_0)$ against $1/[BSA]$ for binding of PDOHBA with BSA (inset shows Benesi–Hildebrand plot of $1/(I-I_0)$ against $1/[BSA]^2$ for binding of PDOHBA with BSA).

may also support the existence of the probe inside the hydrophobic cavity of the albumin. The nonradiative channels assisted by intermolecular hydrogen bonding present in aqueous solution are blocked to a great extent being less effective as the probe binds more and more with protein resulting enhancement of fluorescence intensity and quantum yield values (Table 1).

In order to achieve a quantitative estimation of binding between PDOHBA and BSA, binding constant has been determined from the fluorescence intensity data following the well used Benesi–Hildebrand equation. The complexation reaction with equilibrium constant can be expressed as follows

$$\text{PDOHBA} + \text{BSA} \leftrightarrow \text{PDOHBA} : \text{BSA}$$

$$K = \frac{[PDOHBA : BSA]}{[PDOHBA][BSA]} \tag{4}$$

where K is the binding constant in M^{-1}. The concentration terms of each components of Eq. (4) can be expressed in terms of fluorescence intensity. Assuming that the concentration of the probe–protein complex is very low compared to that of the free protein, the Benesi–Hildebrand relation for these types of complexation process can be written as follows [30,33,34],

$$\frac{1}{(I-I_0)} = \frac{1}{(I_1-I_0)} + \frac{1}{(I_1-I_0)K[BSA]} \tag{5}$$

Table 1
Fluorescence decay times, quantum yield and nonradiative rate constants of PDOHBA in aqueous buffer and in protein media.

Medium	a_1	τ_1 (ns)	a_2	τ_2 (ns)	a_3	τ_3 (ns)	$\langle\tau_{avg}\rangle$ (ns)	χ^2	Φ_F ($\times10^2$)	κ^{nr} (10^{10} s^{-1})
In buffer	0.002	1.019	0.997	0.114	0.001	4.042	0.119	1.076	0.75	0.834
In 5 μM BSA	0.012	0.943	0.003	5.554	0.985	0.119	0.145	1.010	0.99	0.683
In 50 μM BSA	0.155	2.346	0.041	8.431	0.804	0.303	0.954	1.168	1.75	0.103

where I_0, I and I_1 are the emission intensities in absence of, at intermediate and infinite concentration of BSA, respectively. The plot of $1/(I-I_0)$ versus $1/[BSA]$ as depicted in Fig. 2(b) shows linear variation justifying 1:1 complexation between the fluorophore and protein with very high binding constant ($K=(0.67\pm0.05)\times10^4\ M^{-1}$) and discards the probability of 1:2 binding phenomenon (inset of Fig. 2 (b)). From the high value of K; it is evident that PDOHBA binds strongly with BSA. From the determined K value, the free energy change ($\Delta G=$ -RTlnK) for the probe–protein binding process has been calculated to be −21.90 kJ/mol which indicates spontaneous complexation process.

3.3. Steady state fluorescence anisotropy study

Steady-state fluorescence anisotropy (r) study has always occupied a position of central importance in biochemical and biophysical research for its tremendous potential because any factor which affects size, shape, or segmental flexibility of a molecule will affect the observed anisotropy. Since an increase in rigidity of the surrounding environment of a fluorophore reflects in an increase in fluorescence anisotropy, this method can be successfully used in order to locate the probable position of the probe in complex molecular assembly including protein [30,32–35]. From Fig. 3(a), it is noticed that the fluorescence anisotropy value increases gradually with increasing concentration of BSA. The gradual increase in anisotropy of PDOHBA with an increasing protein concentration implies an imposed motional restriction on the fluorophore in the proteinous environment. As depicted in Fig. 3(a), with increasing protein concentration fluorescence anisotropy value increases rapidly at the beginning ([BSA] = 25 μM) and reaches to a maximum ($r=0.21$) at 40 μM of BSA concentration. This indicates that the probe enters into a motionally constrained environment with increasing protein concentration. This high anisotropy value may arise due to strong hydrogen bonding interaction between the amino acid residues of polypeptide backbone of BSA and —OH group of probe PDOHBA.

The measurement of excitation anisotropy is a wavelength sensitive tool which provides a more vivid picture of the surrounding atmosphere of the probe while emitting from the excited state [30,42]. At a particular protein concentration, if the anisotropy increases with the shifting of the excitation wavelength towards red end, then the probe is expected to exist in a motionally restricted environment. As seen in Fig. 3(b), a steady increase in fluorescence anisotropy values with excitation wavelength is observed in case of binding between BSA and PDOHBA at a particular BSA concentration. As the probe binds at the hydrophobic binding site of the protein which is basically motionally confined environment, this increase in anisotropy arises due to slow rates of reorientation of the solvent molecules around the fluorophore in the organized media.

3.4. Acrylamide quenching of PDOHBA-BSA complex

The use of quenchers can help to know the change in the neighboring of the tryptophan residues and their accessibility for quenching molecules. Acrylamide, a well recognized neutral quencher, quenches fluorescence intensity of PDOHBA-BSA complex. A

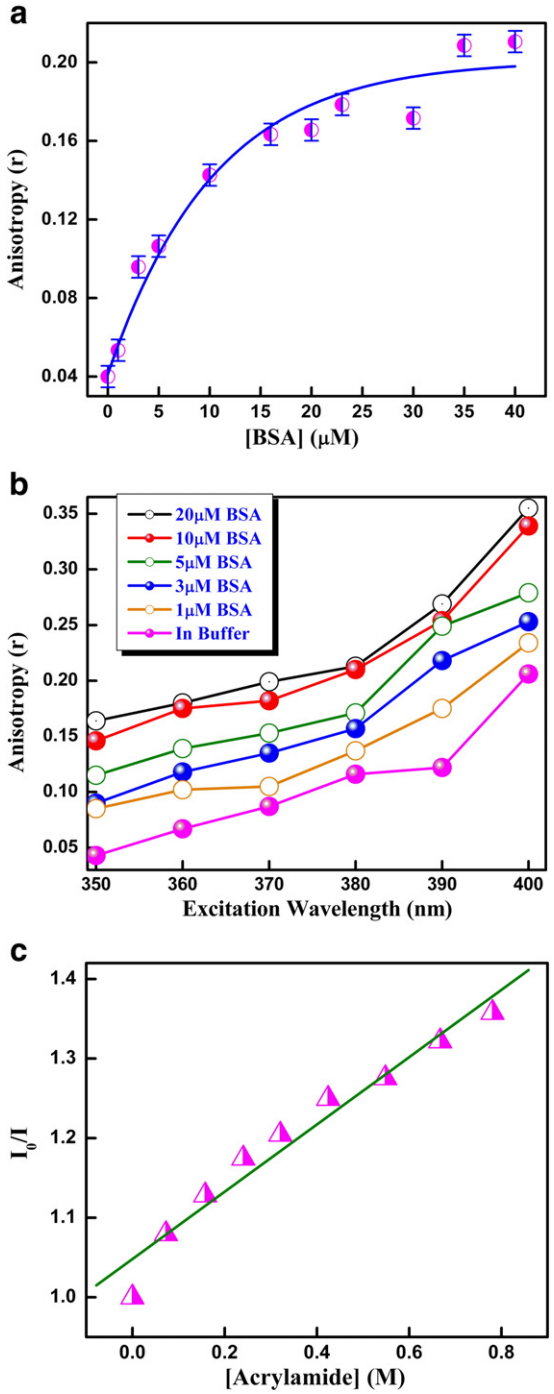

Fig. 3. (a) Variation of steady state fluorescence anisotropy (r) of PDOHBA with increasing concentration of BSA ($\lambda_{ex}=350$ nm, $\lambda_{em}=505$ nm). (b) Variation of steady state anisotropy values ($\lambda_{em}=505$ nm) of PDOHBA with change in excitation wavelength (from 350 nm to 400 nm) at a fixed BSA concentration. (c) Stern–Volmer quenching plot of I_0/I against [acrylamide].

probable explanation for this phenomenon may be the release of probe from the hydrophobic pocket of BSA. The following Stern–Volmer equation is fitted for this quenching phenomenon.

$$\frac{I_0}{I} = 1 + K_{SV}[Q] = 1 + k_q\tau_0[Q] \quad (6)$$

where I_0 and I are the fluorescence intensities of PDOHBA–BSA complex in absence and presence of the quencher (acrylamide), k_q and K_{SV} are the quenching rate constant and Stern–Volmer constant of this complex, τ_0 is the lifetime of PDOHBA–BSA complex in absence of quencher and [Q] is the concentration of the quencher. The plot of I_0/I versus [Acrylamide] is found to be linear (Fig. 3(c)) with K_{SV} and quenching constant (k_q) value of $(0.423 \pm 0.03)\,M^{-1}$ and $(4.43 \pm 0.31) \times 10^8\,M^{-1}\,s^{-1}$, respectively. Acrylamide dispels the probe molecules from hydrophobic interior by approaching close to the binding site of the protein thereby throwing the probe molecules into the aqueous phase. Thus fluorescence of the probe–BSA complex is quenched. The values of K_{SV} and k_q predict that the molecule is deeply embedded in the hydrophobic cavity of BSA.

3.5. Fluorescence time resolved studies

Fluorescence lifetime serves as a sensitive parameter to cast further light on the local environment around a fluorophore in the proteinous media [30,32–35]. Fluorescence decay curves are usually multiexponential in the case of probe–protein binding complexation. In the present case, the decay curves are tri-exponential fitted in order to get best fitted residuals and acceptable χ^2 values (Table 1). As shown in Fig. 4 and Table 1, the lifetime values of PDOHBA in proteinous media are observed to be longer than that which is measured in aqueous buffer solution and increase with increasing protein concentration. The decrease in nonradiative decay rates of the probe in the microheterogeneous environment of protein is reflected by the increase in fluorescence lifetime (Table 1). The nonradiative decay rate constants k^{nr} can be calculated using the following equation:

$$\kappa^{nr} = (1-\Phi_F)/\langle\tau\rangle. \quad (7)$$

It is apparent from Table 1 that the increase in Φ_F and the substantial decrease in κ^{nr} result in an increase in the fluorescence lifetime values. Nonradiative decay channels are operative in the aqueous solution due to hydrogen bonding deactivating channels. Encapsulation of the probe molecules inside the hydrophobic cavity of BSA, where the probe is less exposed to water, decreases its κ^{nr} values and increases its decay times. Stronger binding between BSA and PDOHBA with increase of BSA concentration reduces the probability of deactivation via nonradiative channels and hence fluorescence lifetime value increases.

3.6. Quenching of intrinsic fluorescence of BSA by PDOHBA

Fig. 5 shows the fluorescence and absorption spectra of BSA in absence and presence of PDOHBA at room temperature. The intrinsic fluorescence intensity of BSA decreases gradually with increasing

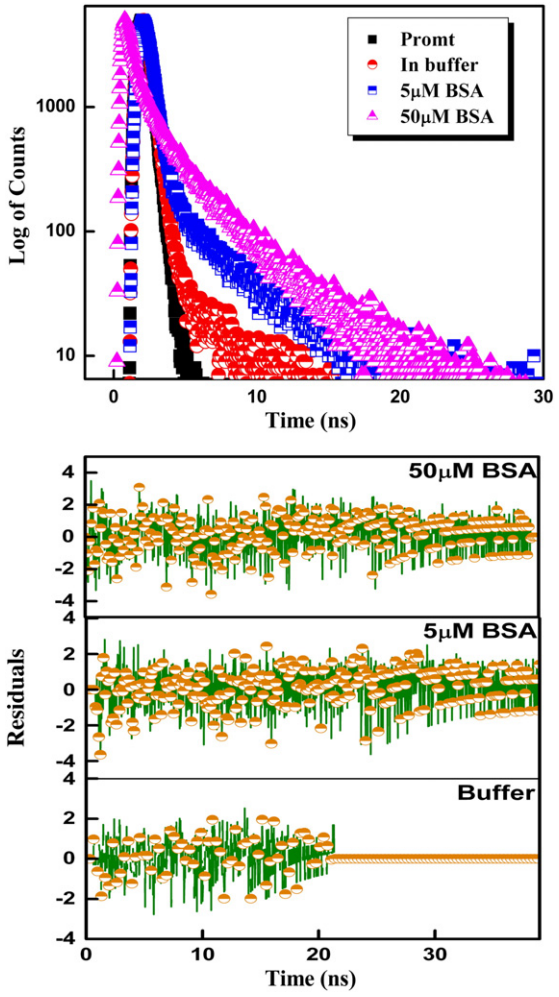

Fig. 4. Fluorescence decay curves of PDOHBA in buffer, 5 μM and 50 μM BSA (λ_{ex} = 340 nm) with best fitted residuals.

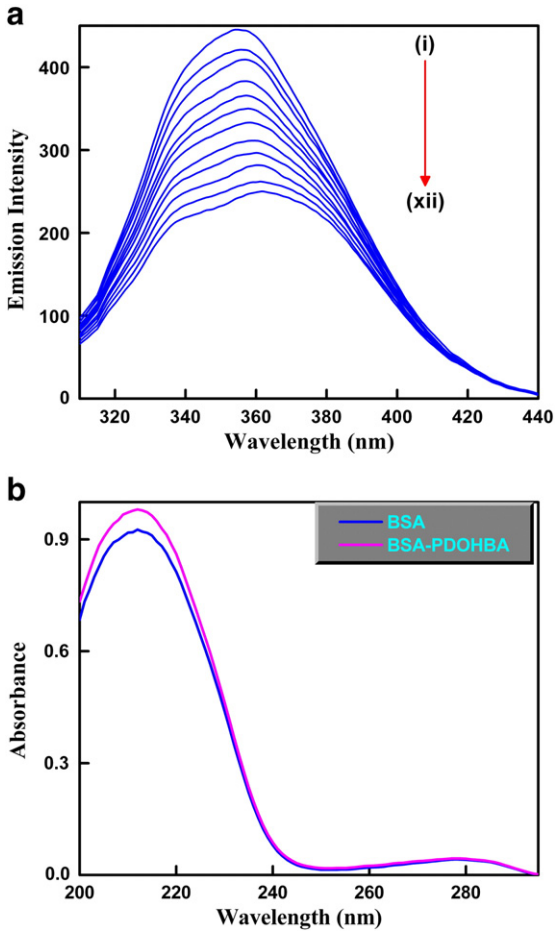

Fig. 5. (a) Fluorescence emission spectra of BSA (5 μM) in presence of various concentrations of PDOHBA (λ_{ex} = 285 nm) at room temperature. Curves i→xii correspond to 0, 0.99, 2.47, 3.92, 5.35, 6.76, 8.15, 9.52, 11.32, 13.08, 14.81 and 16.51 μM concentrations of PDOHBA (b) UV–Vis absorption spectra of BSA (5 μM) and BSA–PDOHBA complex ([BSA] = 5 μM, [PDOHBA] = 5 μM) in 0.01 M Tris buffer.

PDOHBA concentration. Dynamic and static quenching can be recognized by temperature dependence studies [43]. The fluorescence quenching data are analyzed by the Stern–Volmer equation (Eq. 6) at different temperatures (Fig. 6(a)) which depict that they are linear and increasing temperature does not change the linearity of the Stern–Volmer plot indicating the occurrence of a single type of quenching phenomenon, either static or dynamic. It is seen from Table 2 that the K_{SV} as well as k_q values are inversely correlated with temperature, and k_q is much greater than the value of the maximum scatter collision quenching constant (2×10^{10} M^{-1} s^{-1}) [44]. All these results authenticate that the probable quenching mechanism of fluorescence of BSA by PDOHBA is not initiated by dynamic collision but probable by static quenching through the formation of BSA–PDOHBA complex. Difference in the UV–Vis absorption spectra of BSA and BSA–PDOHBA (Fig. 5(b)) also indicates static quenching.

Consequently, the quenching data are analyzed according to following Lehrer equation [45], as the quenching of BSA by PDOHBA originates from the formation of a complex.

$$\frac{I_0}{I_0-I} = \frac{1}{f_a K_a}\cdot\frac{1}{[Q]} + \frac{1}{f_a} \tag{8}$$

In the present case, $(I_0 - I)$ is the difference in fluorescence in the absence and presence of the quencher at concentration [Q], f_a is the fraction of accessible fluorescence and K_a is the effective quenching constant for the accessible fluorophore. The Lehrer plots are shown in Fig. 6(b) and the corresponding quenching constant K_a at different temperatures are listed in Table 2 which again confirms static quenching as K_a value decreases with increase of temperature.

3.7. The binding constant and binding interaction force between BSA and PDOHBA

For the static quenching interaction, if it is assumed that there are similar and independent binding sites in the biomolecule, the equilibrium between free and bound molecules is given by the following modified Stern–Volmer equation:

$$log\frac{I_0-I}{I} = log\, K_b + n\, log[Q] \tag{9}$$

where I_0 and I are the fluorescence intensities of BSA in absence and presence of PDOHBA, K_b and n are the binding constant and number of binding sites, respectively. The binding constant (K_b) as well as the number of binding sites (n) per BSA can be determined from $\log[(I_0 - I)/I]$ versus log[Q] plot. The K_b and n values at different temperatures are listed in Table 2 for PDOHBA associated with BSA. The data clearly shows that K_b decreases with the rising of temperature indicating the formation of an unstable BSA–PDOHBA complex which is in accordance with the trend of K_a as mentioned above (Table 2). On the other hand, the approximate value of n is equal to 1 at different temperatures indicating the existence of just a single binding site in BSA for PDOHBA. Hence, PDOHBA is more likely to bind to the hydrophobic pocket of BSA i.e. to Trp-212 located in subdomain IIA.

The acting forces for binding between ligand and biomolecules include hydrogen bond, van der Walls force, electrostatic and hydrophobic interaction force and so on. To obtain such information for the interaction between BSA and PDOHBA, thermodynamic parameters are calculated from the van't Hoff equation and the corresponding thermodynamic functions are based on temperature effect.

$$ln\, K_b = -\frac{\Delta H}{RT} + \frac{\Delta S}{R} \tag{10}$$

$$\Delta G = \Delta H - T\Delta S = -RT\ In\ K_b \tag{11}$$

ΔH, ΔS, and ΔG are enthalpy change, entropy change and free energy change, respectively, K_b is the binding constant at the corresponding temperature in Kelvin. ΔH and ΔS can be obtained from the plot of $\ln K_b$ versus 1/T, as shown in Fig. 6(c). Ross and Subramanian [46] summed up that the positive ΔH and ΔS values are associated with hydrophobic interaction and negative ΔH and ΔS values are correlated with van der Walls interaction and hydrogen bonding. Finally, electrostatic force usually makes $\Delta H \approx 0$ and $\Delta S > 0$. As can be seen from Table 2, the negative sign for ΔG indicates the spontaneity of binding of PDOHBA with BSA. The positive ΔH (187.5 kJ mol^{-1}) and ΔS (0.517 kJ mol^{-1} K^{-1}) values indicate the presence of less dominating hydrogen bond formation and predominating hydrophobic force between PDOHBA and BSA.

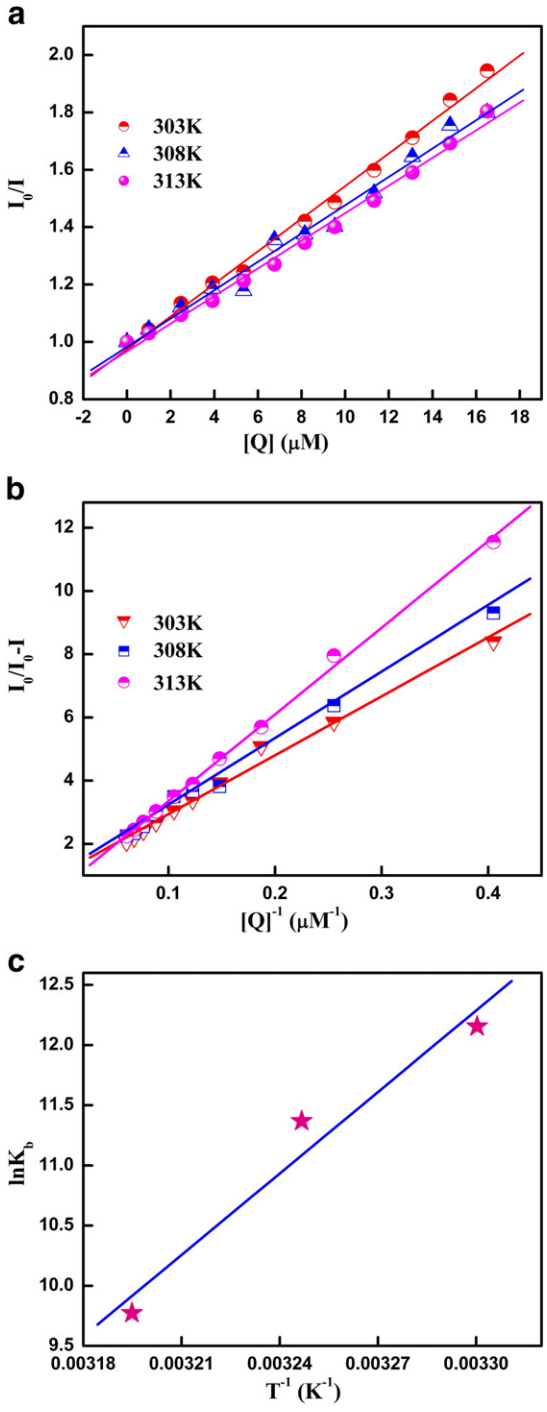

Fig. 6. (a) Stern–Volmer plots and (b) Lehrer plots for the quenching of BSA by PDOHBA at three different temperatures. (c) Van't Hoff plot for binding of BSA with PDOHBA.

Table 2
Quenching and thermodynamic parameters for the interaction of PDOHBA with BSA at different temperatures.

Temperature (K)	K_{sv} ($\times 10^4\ M^{-1}$)	k_q ($\times 10^{12}\ M^{-1}\ s^{-1}$)	K_a ($\times 10^4\ M^{-1}$)	K_b ($\times 10^4\ M^{-1}$)	n	ΔG (kJ mol^{-1})
303	5.683 ± 0.14	5.683 ± 0.14	5.778 ± 0.26	19.01 ± 1.22	1.126	−30.62
308	4.936 ± 0.19	4.936 ± 0.19	5.161 ± 0.18	8.66 ± 0.24	1.040	−29.11
313	4.813 ± 0.13	4.813 ± 0.13	2.229 ± 0.18	1.15 ± 0.12	1.135	−24.33

3.8. Energy transfer from BSA to PDOHBA

Fluorescence resonance energy transfer (FRET) is a non-destructive spectroscopic method that monitors the close proximity and relative angular orientation of fluorophores. The donor and acceptor molecules can be entirely separated or attached to the same macromolecule. According to Förster, the efficiency of FRET depends on the relative orientation of the donor and acceptor dipoles, the extent of overlap between the donor emission and the acceptor absorption and the distance between the donor and acceptor [47]. In the present case overlap between the donor emission and the acceptor absorption is very good (figure not given). The energy transfer efficiency (E) is related not only to the distance (r) between the acceptor and the donor but also to the critical energy transfer distance or Förster radius (R_0), that is

$$E = \frac{R_0^6}{R_0^6 + r^6} = 1 - \frac{I}{I_0} \tag{12}$$

where I and I_0 are the fluorescence intensities of the donor in presence and absence of the probe, respectively. R_0 is calculated as

$$R_0 = 9.78 \times 10^3 \left[\kappa^2 . n^{-4} . \Phi_D . J(\lambda)\right]^{1/6} \tag{13}$$

where Φ_D is the fluorescence quantum yield of the donor in the absence of the acceptor, κ^2 is the dipole orientation factor involving the geometry of the donor–acceptor dipoles, and n is the refractive index of the medium. The spectral overlap integral J is calculated as follows,

$$J = \frac{\int_0^\infty I_D(\lambda).\varepsilon_A(\lambda).\lambda^4.d\lambda}{\int_0^\infty I_D(\lambda).d\lambda} \tag{14}$$

where I_D is the normalized donor emission spectrum and ε_A is the acceptor molar extinction coefficient.

Using the values of $\kappa^2 = 2/3$, n = 1.333, and $\Phi_D = 0.15$, we can calculate that $J = 1.362 \times 10^{-16}\ cm^3\ l\ mol^{-1}$ from the overlapped region, E = 0.46, R_0 = 1.26 nm and r = 1.30 nm. The average distance between PDOHBA and BSA is very small (<8 nm) suggesting that the nonradiative energy transfer from BSA to PDOHBA occurs with high probability and the result $r > R_0$ again indicates the presence of static quenching interaction between PDOHBA and BSA. It also infers that the probe binds to the hydrophobic zone of BSA and energy transfer occurs between Trp-212 and probe. This method of distance measurement for BSA may be confusing because of the presence of two tryptophan residues (Trp-212 and Trp-134) in BSA. But from previous studies, it is already known to us that Trp-134 is more exposed to aqueous phase and its fluorescence characteristics are quite different to that of Trp-212 [2]. But, as argued in Section 3.2, with a view to the hydrophobic nature of the probe, it is likely that the probe binds to a hydrophobic binding pocket of BSA, i.e., in domain II or III. Since domain III does not contain any tryptophan residue, it is presumed that Trp-212, in domain II, is the donor moiety of the present FRET process.

3.9. The effect of PDOHBA on the configuration of BSA

Synchronous fluorescence spectroscopy introduced by Lloyd [48] can provide information about the molecular environment in the vicinity of a chromophore under physiological condition by involving the simultaneous scanning of excitation and emission monochromators of a fluorimeter, while maintaining a fixed wavelength difference ($\Delta\lambda$) between them. Vekshin et al. [49] suggested that the shift in wavelength of the emission maxima λ_{max} corresponds to the changes of polarity around the chromophore molecule. The synchronous fluorescence spectra only show the tyrosine and tryptophan residues of BSA when the wavelength interval ($\Delta\lambda$) is fixed at 15 nm and 60 nm, respectively. The synchronous fluorescence spectra of tyrosine and tryptophan residues of BSA at various concentrations of PDOHBA are shown in Fig. 7. Comparing Fig. 7(a) and (b) we can easily conclude that the fluorescence of BSA is mainly originated from that of tryptophan residues. It is apparent from Fig. 7(a) that when $\Delta\lambda$ is set at 15 nm, the maximum emission wavelength shows 3 nm blue shift at the investigated concentration range and when $\Delta\lambda = 60$ nm, the maximum emission wavelength undergoes a blue shift of 4 nm from

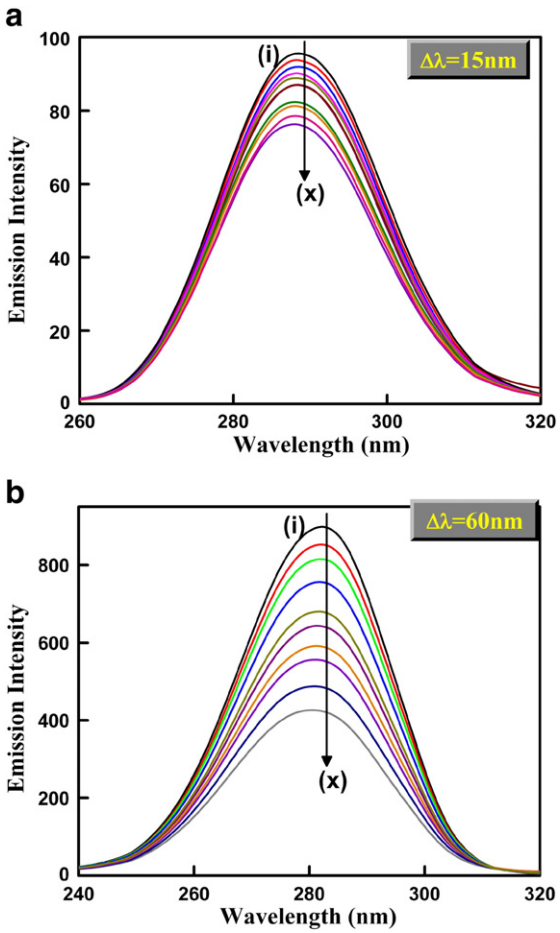

Fig. 7. Synchronous fluorescence spectra of BSA (5 μM) with increasing concentration of PDOHBA (i → x, [PDOHBA] = 0, 0.99, 2.47, 3.92, 5.35, 8.15, 9.52, 11.32, 14.81, and 16.51 μM) with (a) $\Delta\lambda = 15$ nm and (b) $\Delta\lambda = 60$ nm.

283 nm to 279 nm (Fig. 7(b)). The blue shift of the emission maximum indicates that the conformation of BSA is altered and the polarity around the tryptophan and tyrosine residues is decreased and the hydrophobicity is increased in presence of PDOHBA.

The three dimensional fluorescence spectroscopy can give additional information or evidence regarding the conformational changes of BSA in presence of PDOHBA. The three dimensional fluorescence spectra of BSA and BSA–PDOHBA are shown in Fig. 8(a) and (b), respectively and it is found that three dimensional fluorescence map of BSA and BSA–PDOHBA are different. Two typical fluorescence peaks (peak I and peak II) could be easily found in the three dimensional fluorescence spectra in the lower right of the first-ordered Rayleigh scattering peak (A, $\lambda_{ex} = \lambda_{em}$) and left of the second ordered Rayleigh scattering peak (B, $\lambda_{em} = 2\lambda_{ex}$). Peak I mainly reveals the spectral behavior of tryptophan and tyrosine residues as BSA is excited at 280 nm. From the UV–Vis absorption spectra of BSA (Fig. 5(b)), it is seen that there is an absorption peak at ~277 nm arising by the $\pi \rightarrow \pi^*$ transition of aromatic amino acids in BSA as the tryptophan, tyrosine and phenylalanine in the binding cavity of protein have conjugated π electrons thereby forming charge transfer complex with other electron absence or π-electronic systems [50]. Moreover, besides peak I, there is another new fluorescence peak (peak II). The excitation wavelength of this peak is 230 nm and BSA has strong absorption peak at 212 nm (Fig. 5(b)). Considering these two phenomena, it can be inferred that peak II is mainly originated by $n \rightarrow \pi^*$ transition of BSA with characteristic polypeptide backbone structure. The detailed changes of the characteristic parameters are summarized in Table 3. The decrease of the fluorescence intensity of the two peaks of BSA and the blue shifting of the maximum emission wavelength after addition of PDOHBA suggest that a less polar environment of both residues which is consistent with the results of synchronous fluorescence spectra (Fig. 7). Thus we may conclude that

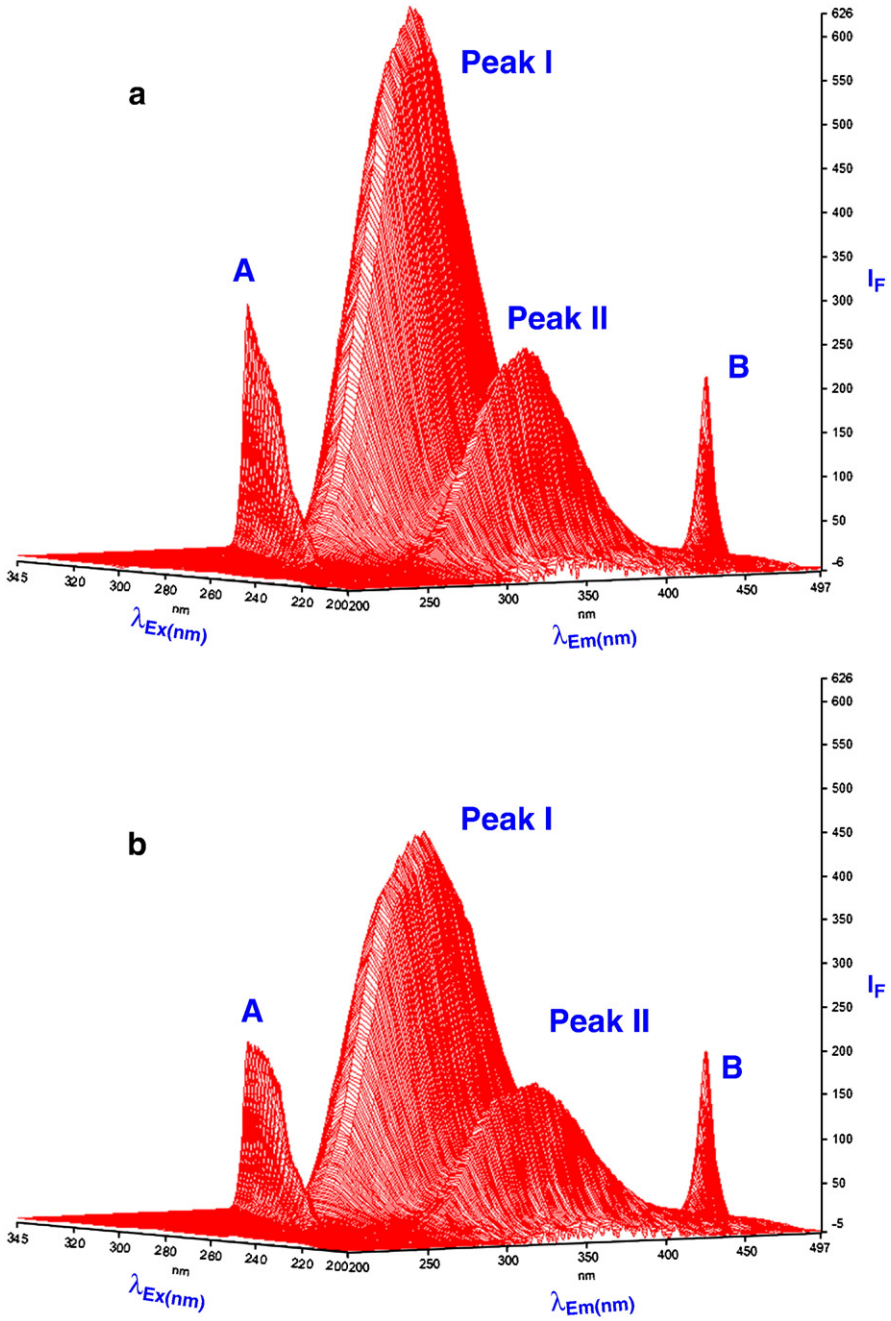

Fig. 8. Three dimensional fluorescence spectra of (a) BSA (5 μM) and (b) BSA–PDOHBA complex ([BSA] = 5 μM, [PDOHBA] = 5 μM).

Table 3
Some characteristic parameters obtained from three dimensional fluorescence spectra of BSA and BSA–PDOHBA systems.

System	Peak I ($\lambda_{ex}/\lambda_{em}$)	Δλ (nm)	Intensity	Peak II ($\lambda_{ex}/\lambda_{em}$)	Δλ (nm)	Intensity	Intensity ratio
BSA	280/362	82	613.35	230/358	128	250.66	2.45:1
BSA–PDOHBA	260/355	95	441.85	230/354	124	163.62	2.70:1

addition of PDOHBA changes the polarity of the microenvironment and thus results the conformational changes of BSA.

So to get deeper insight on the structural changes of BSA by the addition of PDOHBA, circular dichroism (CD) experiment is carried out and the results are shown in Fig. 9. The CD spectrum of BSA alone exhibits two negative peaks at 208 nm and 222 nm which are contributed from $n \rightarrow \pi^*$ transition of the peptide inter linkage of α-helix [51]. With addition of PDOHBA, there occurs only a decrease in band intensity without any significant shift of the peaks outlining that the probe induces a slight decrease in the helix content of the protein. The α-helix content of BSA can be estimated according to the following equation [52]:

$$\%\alpha - HelixContent = \frac{\theta_{MRD} - 4000}{33000 - 4000} * 100 \quad (15)$$

where, θ_{MRD} is the mean residue ellipcity at 208 nm in deg.cm^2.d mol^{-1}. It can be calculated as follows:

$$\theta_{MRD} = \frac{\theta_D(m\ deg)M}{10CLN_r} \quad (16)$$

where θ_D is the observed CD (mdeg) obtained in experiment, M is the molecular weight of BSA in Da, C is the BSA concentration (mg ml^{-1}), L is the sample cell path length and N_r is the number of amino acid residues. BSA has a molecular weight of 66,200 Da with 583 amino acid residues [13]. According to the above equations, the %α-helix content of BSA is estimated and it decreases from 47.31% (in absence of PDOHBA) to 41.71% (in presence of PDOHBA) as shown in Fig. 9. The decrease of α-helix content points towards the fact that PDOHBA combines with the amino acid residues of the main polypeptide chain of protein and perturbs interior electrostatic networks. On the basis of the discussion of synchronous and three dimensional fluorescence spectra and CD spectra it can be easily concluded that PDOHBA interacts with BSA by causing slight unfolding of the polypeptide of protein and conformational changes.

3.10. Surfactant induced uncoiling of protein

It is well known that the intrinsic fluorescence intensity of tryptophan of BSA decreases gradually with addition of SDS. Similar to the previous reports [18–23], the binding isotherm of BSA with surfactant shows four characteristic regions (A, B, C, and D) (Figure not given). The region (C) is the most significant one due to cooperative interaction with the formation of "*pearl and necklace*" [23] structure of BSA–surfactant complex where a massive increase in binding of SDS to BSA takes place because of cooperative interactions resulting in SDS induced unfolding of BSA (Scheme 2).

The quenching of intrinsic fluorescence of BSA by SDS can also be analyzed according to the Stern–Volmer Eq. 6. We have used modified Stern–Volmer Eq. 9 for the determination of binding constant (K_b) and binding affinities (n). A plot of $\log[(I_0 - I)/I]$ against log[SDS] has been shown in Fig. 10(a). This figure also authenticates that the binding of SDS to BSA takes place by traveling the four regions A–D. The values of K_{SV}, K_b, n, and ΔG have been estimated for the region A–C using Eqs. 6, 9 and 11 and have been summarized in Table 4. The Stern–Volmer plot for the region A and the modified Stern–Volmer plot for the region C have been shown in Fig. 10(b) and inset of Fig. 10 (b), respectively. The values of K_b and ΔG of region C indicate that binding of SDS with BSA in this region is not only spontaneous but also occurs very strongly. The magnitude of n also concludes strong binding nature of SDS in this concentration range. These parameters corresponding to the region B where non-cooperative binding occur, are found to be very small as compared to that of regions A and C.

The plot of emission intensity of PDOHBA–BSA complex against SDS concentration is shown in Fig. 11. Here also the curve can be divided into four distinct regions. The most important part of SDS–BSA interaction after region B is termed as the cooperative region where emission intensity sharply increases which is similar to that of the observation in case of protein–SDS binding curve [18–23]. This indicates that massive binding of the surfactant begins to occur on the protein leading to its uncoiling process. Due to unfolding of BSA, the number of hydrophobic binding sites increases (Table 4). So the

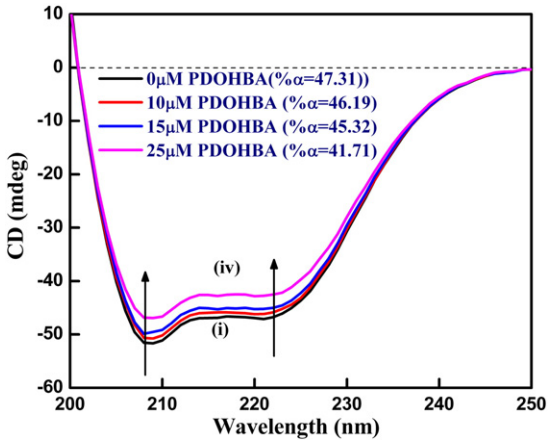

Fig. 9. Circular dichroism spectra of BSA (5 μM) with increasing concentration of PDOHBA ([PDOHBA] = 0, 10, 15, and 25 μM).

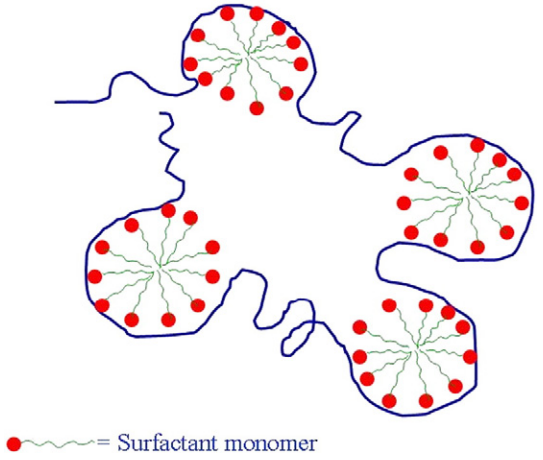

Scheme 2. Schematic representation of the pearl and necklace model of interaction between BSA and surfactants.

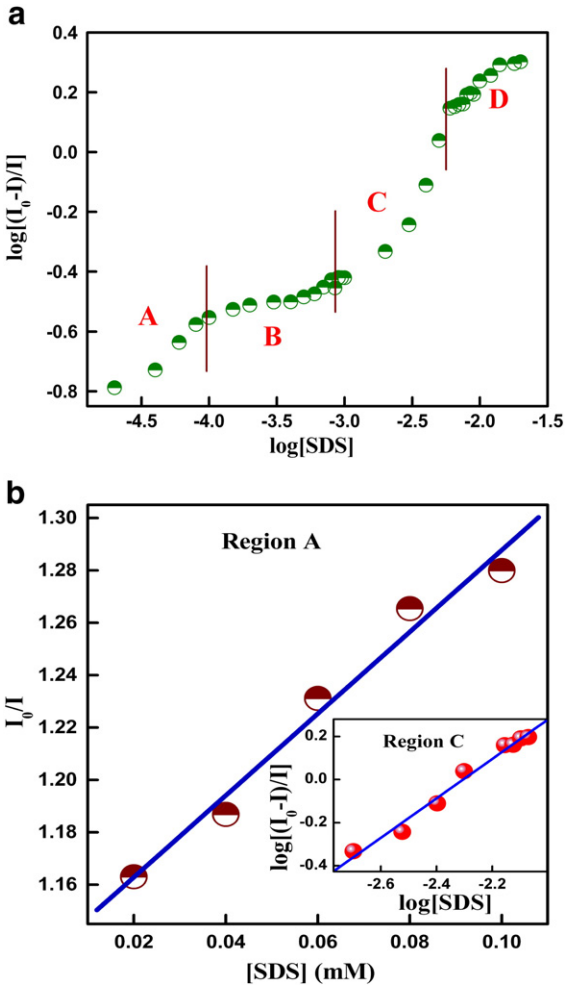

Fig. 10. (a) A plot of $\log[(I_0-I)/I]$ versus log[SDS] for the interaction between BSA (20 μM) and SDS showing four regions of binding. (b) Stern–Volmer plot of region A representing a concentration range 0–0.1 mM SDS, (inset shows modified Stern–Volmer plot of region C representing a concentration range 2–8 mM SDS).

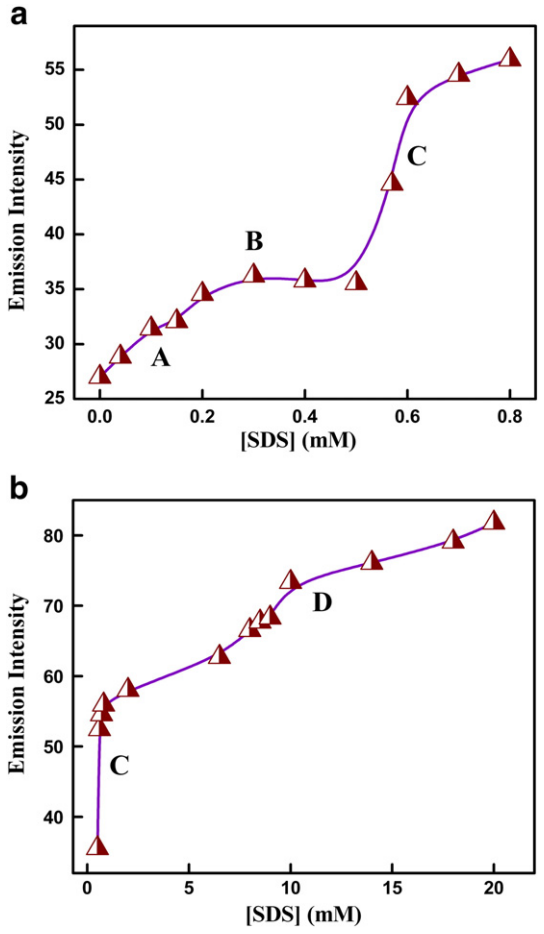

Fig. 11. Variation of emission intensity (at 505 nm) of PDOHBA (6 μM) bound to BSA (20 μM) with increasing concentration of SDS from 0 mM to (a) 0.8 mM and (b) 20 mM.

emission intensity increases as the probe molecule gets more and more solubilization in the hydrophobic region and senses increasing hydrophobicity of its surrounding environment. After region C, with increasing SDS concentration, insignificant change in emission intensity indicates that further binding of the surfactant does not occur on the protein at saturation region D. The emission intensity of PT band of PDOHBA increases with increase of SDS concentration as the probe and SDS both have affinity towards BSA. So PDOHBA can be endorsed to the competitive nature of binding between SDS and PDOHBA towards BSA. Since the plots shown in Fig. 11 replicate well with the binding isotherm of BSA–SDS interaction (Fig. 10(a)), it can be easily concluded that the variation of the fluorescence intensity of the PT band of PDOHBA reflects its solubilization in the hydrophobic region of BSA–SDS aggregates and matches well with the nature of protein–surfactant interaction.

Table 4
Stern–Volmer quenching constants and binding parameters for the interaction of SDS with BSA at different regions.

Region	K_{SV} ($\times 10^3$ M^{-1})	K_b ($\times 10^4$ M^{-1})	N	ΔG (kJ mol^{-1})
A	1.561 ± 0.13	0.736 ± 0.11	0.36	−22.44
B	0.137 ± 0.01	0.207 ± 0.09	0.24	−19.24
C	0.184 ± 0.01	12.83 ± 1.30	0.92	−29.64

3.11. Effect of urea on denaturation of protein

Denaturation does not affect the primary structure of protein but it disrupts both the secondary and tertiary structures of proteins i.e. total or partial loss of three dimensional structures. Proteins can be denatured by heat, pH or chemical denaturants such as urea, a well known chaotropic denaturant [30,32–35]. After finding the binding interaction between BSA and PDOHBA, we intend to see the effect of chaotropes on this binding interaction. As seen in Fig. 12, on gradual addition of urea (0–9 M) to the protein bound probe, the emission

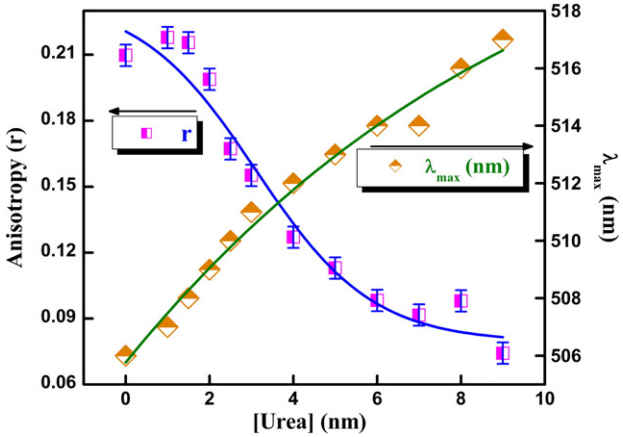

Fig. 12. Plot of emission maxima (λ_{max}) and fluorescence emission anisotropy (r) values as a function of added urea ([BSA] = 20 μM, [PDOHBA] = 6 μM).

maximum undergoes a progressive red shift along with a decrease in fluorescence anisotropy. The red shift and decrease in fluorescence anisotropy indicate that the polarity of the microenvironment around the probe increases. As the protein structure gets disrupted due to addition of denaturant, the probe molecules encapsulated within the hydrophobic cavity of native BSA are exposed to the aqueous phase. Fig. 12 with a pattern opposite to that of Fig. 2(a) and 3(a) reflects that probe–protein binding is weakened with the addition of urea resulting greater exposure of the probe molecules into the aqueous phase than that in proteinous hydrophobic environment. So the probe PDOHBA well documented the urea induced denaturation of protein BSA.

3.12. Destructive and protective actions of SDS on urea denatured protein

Urea is a stronger denaturant of protein than SDS as urea completely destroys the helicity of BSA. On the other hand, SDS plays dual character—destructive for native conformation and protective for urea-denatured protein. Hence coexistence of urea and SDS leads to a competitive denaturation process. This dual function of SDS can be shown in three different regions of urea concentration—(1) below 3 M urea, denaturation of protein takes place by SDS, not by urea, (2) between 4 and 8 M, urea denatured protein is refolded by SDS at low concentration, then further addition of SDS results in denaturation of protein and (3) above 8 M urea, only increase of helicity of BSA can take place.

It has been previously observed that the emission maximum of the PT band of PDOHBA is shifted from ~506 nm in BSA to ~517 nm in presence of 9 M urea (Fig. 12). Denaturation of protein by urea expels the probe to the bulk aqueous phase thereby exhibiting less hydrophobic interaction. At a particular urea concentration, the variations of the emission maxima of the probe in protein environment with the variation of the SDS concentration have been shown in Fig. 13. At [urea] = 2 M, the emission band shifts from ~506 nm to ~513 nm up to 1 mM SDS concentration as SDS acts as destabilizer of protein thereby showing red shift and then attains a constancy (Fig. 13(a)). As seen in Fig. 13(b), at the initial low concentration of SDS, the emission maximum undergoes a blue shift due to recoiling of BSA and then there occurs a sharp rise of λ_{max} indicating greater exposure of the probe to aqueous phase. Fig. 13(c) clearly exhibits the increase in helicity of BSA with the addition of surfactant in 9 M urea-denatured protein. So the conformational change of BSA i.e. helicity of protein can be categorically monitored by using PDOHBA as an extrinsic probe.

4. Conclusion

The present work reports the study of interaction of fluorescence probe para-N,N-dimethylamino orthohydroxy benzaldehyde (PDOHBA) with BSA and the potential use of this extrinsic probe as reporter for folding, unfolding and refolding of protein. Steady state and time resolved fluorescence along with fluorescence anisotropy, acrylamide quenching phenomenon as well as fluorescence energy transfer point towards the *locking in* of the probe in hydrophobic pocket of the protein secondary structure. From fluorescence quenching and CD measurement it is found that probe–protein interaction induces slight unfolding of the constitutive polypeptides of protein resulting in a conformational change of it thereby causing greater exposure of some hydrophobic regions. Binding isotherm between BSA and SDS proposes that the uncoiling of protein by SDS takes place by formation of micelle-like aggregate by wrapping around them (*pearl and necklace model*). This probe can also be utilized to study the destructive and protective actions of SDS micelle on the urea-denatured protein BSA.

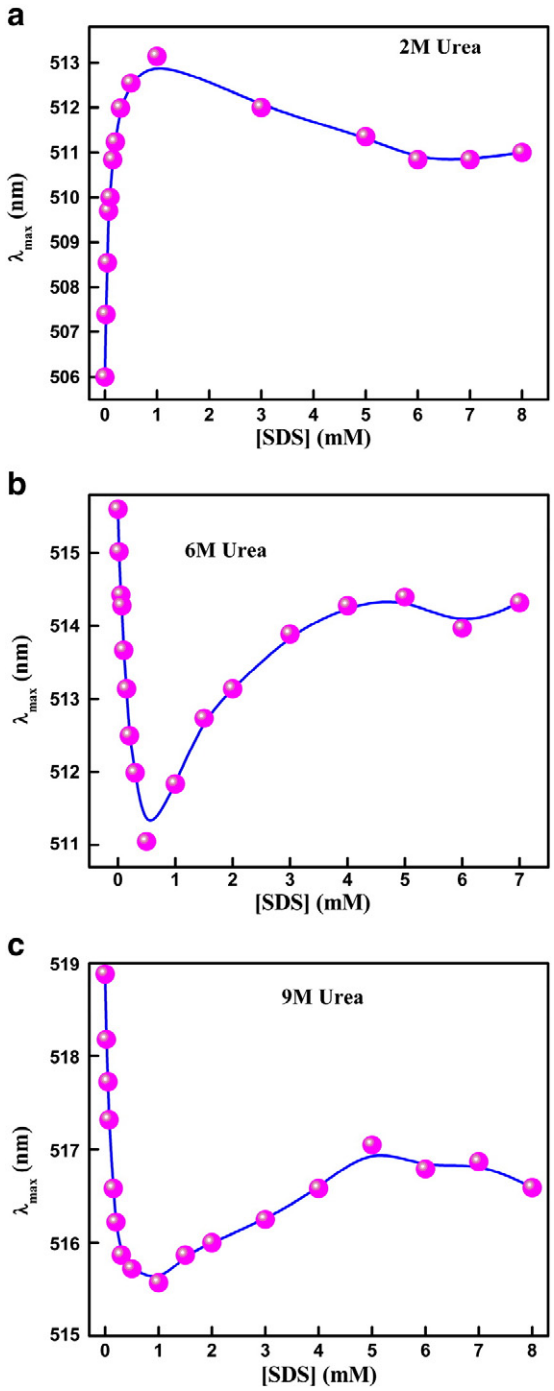

Fig. 13. Plot of emission maxima of BSA–PDOHBA complex (λ_{ex} = 340 nm, λ_{em} = 505 nm) versus SDS concentration in (a) 2 M, (b) 6 M and (c) 9 M urea solution ([BSA] = 20 μM, [PDOHBA] = 6 μM).

Acknowledgments

NG gratefully acknowledges DST, India (Project No. SR/S1/PC/26/2008) for financial support. AS and BKP thank CSIR, New Delhi for SRF fellowship. We appreciate the cooperation received from Prof. T. Ganguly and Dr. P. K. Das of IACS, Kolkata for their kind help in lifetime measurements and CD study respectively.

References

[1] D.C. Carter, J.X. Ho, Structure of serum albumin, Adv. Protein Chem. 45 (1994) 153–203.

[2] Y. Moriyama, D. Ohta, K. Hadiya, Y. Mitsui, K. Takeda, Fluorescence behavior of tryptophan residues of bovine and human serum albumins in ionic surfactant solutions: a comparative study of the two and one tryptophan(s) of bovine and human albumins, J. Protein Chem. 15 (1996) 265–272.
[3] J.K. Choi, J. Ho, S. Curry, D. Qin, R. Bittman, J.A. Hamilton, Interactions of very long-chain saturated fatty acids with serum albumin, J. Lipid Res. 43 (2002) 1000–1010.
[4] S. Makino, J.A. Reynolds, C. Tanford, The binding of deoxycholate and Triton X-100 to proteins, J. Biol. Chem. 248 (1973) 4926–4932.
[5] Y. Zhang, D.E. Wilcox, Thermodynamic and spectroscopic study of CuII and NiII binding to bovine serum albumin, J. Biol. Inorg. Chem. 7 (2002) 327–337.
[6] K. Kamikubo, S. Sakata, S. Nakamura, T. Komaki, K. Miura, Thyroxine binding to human serum albumin immobilized on sepharose and effects of nonprotein albumin-binding plasma constituents, J. Protein Chem. 9 (1990) 461–465.
[7] B. Sengupta, P.K. Sengupta, The interaction of quercetin with human serum albumin: a fluorescence spectroscopic study, Biochem. Bioph. Res. Co. 299 (2002) 400–403.
[8] X.Z. Feng, Z. Liu, L.J. Yang, C. Wang, C.L. Bai, Investigation of the interaction between acridine orange and bovine serum albumin, Talanta 47 (1998) 1223–1229.
[9] S. Chatterjee, T.S. Srivastava, Spectral investigations of the interaction of some porphyrins with bovine serum albumin, J. Porphyr. Phthalocya. 4 (2000) 147–157.
[10] Y.J. Hu, Y. Liu, J.B. Wang, et al., Study of the interaction between monoammonium glycyrrhizinate and bovine serum albumin, J. Pharmaceut. Biomed. 36 (2004) 915–919.
[11] Y.Q. Wang, H.M. Zang, G.C. Zang, et al., Interaction of the flavonoid hesperidin with bovine serum albumin: a fluorescence quenching study, J. Pharmaceut. Biomed. 43 (2007) 1869–1875.
[12] T. Peters, Serum albumin, Adv. Protein Chem. 37 (1985) 161–245.
[13] J.F. Foster, Albumin Structure, Function and Uses; Pergamon Press, Oxford, UK, 1977.
[14] A. Papadopoulou, R.J. Green, R.A. Frazier, Interaction of flavonoids with bovine serum albumin: a fluorescence quenching study, J. Agr. Food Chem. 53 (2005) 158–163.
[15] V. Daggett, A. Fersht, The present view of the mechanism of protein folding, Nat. Rev. Mol. Cell Bio. 4 (2003) 497–502.
[16] G. Taubes, Misfolding the way to dise, Science 271 (1996) 1493–1495.
[17] C.M. Dobson, Principles of protein folding, misfolding and aggregation, Semin. Cell Dev. Biol. 15 (2004) 3–16.
[18] E.D. Goddard, Interaction of surfactant with polymers and proteins, Protein–Surfactant Interactions, CRC Press, Boca Raton, New York, 1993.
[19] C. Tanford, The Hydrophobic Effect: Formation of Micelles and Biological Membranes, 2nd ed Wiley-Interscience, New York, 1980.
[20] S. Shingawa, M. Sato, K. Kameyama, T. Takagi, Effect of salt concentration on the structure of protein-sodium dodecyl sulfate complexes revealed by small-angle X-ray scattering, Langmuir 10 (1994) 1690–1694.
[21] J. Oakes, Protein–surfactant interactions. Nuclear magnetic resonance and binding isotherm studies of interactions between bovine serum albumin and sodium dodecyl sulphate, J. Chem. Soc., Faraday Trans. 1 70 (1974) 2200–2209.
[22] N.J. Turro, X.-G. Lei, K.P. Ananthapadmanabhan, M. Aronson, Spectroscopic probe analysis of protein–surfactant interactions: the BSA/SDS system, Langmuir 11 (1995) 2525–2533.
[23] X.H. Guo, N.M. Zhao, S.H. Chen, J. Teixeira, Small-angle neutron scattering study of the structure of protein/detergent complexes, Biopolymers 29 (1990) 335–346.
[24] M.M. Bradford, A rapid and sensitive method for the quantitation of microgram quantities of protein utilizing the principle of protein–dye binding, Anal. Biochem. 72 (1976) 248–254.
[25] O.H. Lowry, N.J. Rosebrough, A.L. Farr, R.J. Randall, Protein measurement with the folin-phenol reagents, J. Biol. Chem. 193 (1951) 265–275.
[26] F. Joseph, The biuret method of estimating albumin and globulin in serum and urine, Biochem. J. 29 (1935) 799–803.
[27] G.M. Edelman, W.O. Mcclure, Fluorescent probes and the conformation of proteins, Acc. Chem. Res. 1 (1968) 65–70.
[28] L. Brand, J.R. Gohlke, Fluorescence probes for structure, Annu. Rev. Biochem. 41 (1972) 843–868.
[29] A.P. Demchenko, Topics in Fluorescence Spectroscopy: Biochemical Applications, Plenum, New York, 1992.
[30] R.B. Singh, S. Mahanta, A. Bagchi, N. Guchhait, Interaction of human serum albumin with charge transfer probe ethyl ester of N, N-dimethylamino naphthyl acrylic acid: an extrinsic fluorescence probe for studying protein micro-environment, Photochem. Photobiol. Sci. 8 (2009) 101–110.
[31] R.B. Singh, S. Mahanta, N. Guchhait, Destructive and protective action of sodium dodecyl sulphate micelles on the native conformation of bovine serum albumin: a study by extrinsic fluorescence probe 1-hydroxy-2-naphthaldehyde, Chem. Phys. Lett. 463 (2008) 183–188.
[32] S. Mahanta, R.B. Singh, N. Guchhait, Study of proteinâ€"probe interaction and protective action of surfactant sodium dodecyl sulphate in urea-denatured HSA using charge transfer fluorescence probe methyl ester of N, N-dimethylamino naphthyl acrylic acid, J. Fluoresc. 19 (2009) 291–302.
[33] S. Ghosh, N. Guchhait, Chemically induced unfolding of bovine serum albumin by urea and sodium dodecyl sulfate: a spectral study with the polarity-sensitive charge-transfer fluorescent probe (E)-3-(4-methylaminophenyl)acrylic acid methyl ester, Chem. Phys. Chem. 10 (2009) 1664–1671.
[34] B.K. Paul, A. Samanta, N. Guchhait, Exploring hydrophobic subdomain iia of the protein bovine serum albumin in the native, intermediate, unfolded, and refolded states by a small fluorescence molecular reporter, J. Phys. Chem. B 114 (2010) 6183–6196.
[35] A. Mallick, B. Halder, N. Chattopadhyay, Spectroscopic investigation on the interaction of ICT probe 3-acetyl-4-oxo-6,7-dihydro-12H Indolo-[2,3-a] quinolizine with serum albumins, J. Phys. Chem. B 109 (2005) 14683–14690.
[36] S. Mahanta, R.B. Singh, S. Kar, N. Guchhait, Evidence of coupled photoinduced proton transfer and intramolecular charge transfer reaction in para-N, N-dimethylamino orthohydroxy benzaldehyde: spectroscopic and theoretical studies, Chem. Phys. 354 (2008) 118–129.
[37] M. Fischer, J. Georges, Fluorescence quantum yield of rhodamine 6G in ethanol as a function of concentration using thermal lens spectrometry, Chem. Phys. Lett. 260 (1996) 115–118.
[38] P. Mandal, S. Kundu, T. Misra, S.K. Roy, T. Ganguly, Effects of liquid crystal environment on the spectroscopic and photophysical properties of well-known reacting systems 2,3-dimethylindole (DMI) and 9-cyanoanthracene (9CNA), J. Phys. Chem. A 111 (2007) 11480–11486.
[39] S. Dahne, W. Freyer, K. Teuchner, J. Dobkowski, Z.R. Grabowski, Dual and multiple fluorescence mechanisms of p-dimethylaminobenzaldehyde and its trimethylene-bridged double molecule, J. Lumin. 22 (1980) 37–49.
[40] J. Catalan, F. Toriblo, A.U. Acuna, Intramolecular hydrogen bonding and fluorescence of salicylaldehyde, salicylamide, and o-hydroxyacetophenone in gas and condensed phase, J. Phys. Chem. 86 (1982) 303–306.
[41] A. Samanta, B.K. Paul, S. Mahanta, R.B. Singh, S. Kar, N. Guchhait, Evidence of acid mediated enhancement of photoinduced charge transfer reaction in 2-methoxy-4-(N, N-dimethylamino)benzaldehyde: spectroscopic and quantum chemical study, J. Photochem. Photobiol. A Chem. 212 (2010) 161–169.
[42] A. Chattopadhyay, S. Mukherjee, Fluorophore environments in membrane-bound probes: a red edge excitation shift study, Biochemistry 32 (1993) 3804–3811.
[43] J.R. Lackowicz, Principles of Fluorescence Spectroscopy, 3rd ed. Plenum Press, New York, 2006.
[44] R.E. Maurice, A.G. Camillo, Fluorescence quenching studies with proteins, Anal, Biochem. 114 (1981) 199–212.
[45] S.S. Lehrer, Solute perturbation of protein fluorescence quenching of the tryptophyl fluorescence of model compounds and of lysozyme by iodide ion, Biochemistry 10 (1971) 3254–3263.
[46] P.D. Ross, S. Subramanian, Thermodynamics of protein association reactions: forces contributing to stability, Biochemistry 20 (1981) 3096–3102.
[47] T. Förster, Transfer mechanisms of electronic excitation, Discuss. Faraday Soc. 27 (1959) 7–17.
[48] J.B.F. Lloyd, Synchronized excitation of fluorescence emission spectra, Nature 231 (1971) 64–65.
[49] N.L. Vekshin, Separation of the tyrosine and tryptophan components of fluorescence using synchronous scanning method, Biofizika 41 (1996) 1176–1179.
[50] J. Kang, Y. Liu, M.X. Xie, S. Li, M. Jiang, Y.D. Wang, Interactions of human serum albumin with chlorogenic acid and ferulic acid, Biochim. Biophys. Acta 1674 (2004) 205–212.
[51] P. Yang, F. Gao, The Principle of Bioinorganic Chemistry, Science Press, 2002.
[52] N. Greenfield, G.D. Fasman, Computed circular dichroism spectra for the evaluation of protein conformation, Biochemistry 8 (1969) 4108–4116.